

Brought to you by:
Australian National University LibraryLogin: Register

Home Browse Search My Settings Alerts Help

Quick Search Title, abstract, keywords

Author e.g. j s smith



Journal/book title

Volume

Issue

Page

Clear

Earth and Planetary Science Letters

Volume 254, Issues 1-2, 15 February 2007, Pages 214-226

Summary [Full Text + Links](#) [PDF \(2610 K\)](#) [View thumbnail images](#) | [View full size images](#)
 Add to my Quick Links
 Cited By
 E-mail Article
 Save as Citation Alert
 Export Citation
 Citation Feed
doi:10.1016/j.epsl.2006.11.037 Cite or Link Using DOI

Copyright © 2006 Elsevier B.V. All rights reserved.

Asteroid mega-impacts and Precambrian banded iron formations: 2.63 Ga and 2.56 Ga impact ejecta/fallout at the base of BIF/argillite units, Hamersley Basin, Pilbara Craton, Western Australia

Andrew Glikson and John Vickers

aDepartment of Earth and Marine Science and the Planetary Research Institute, Australian National University, Canberra, A.C.T. 0200, Australia

Received 23 September 2006; revised 1 November 2006; accepted 18 November 2006. Editor: G.D. Price. Available online 28 December 2006.

Abstract

The temporal association between late Archaean to earliest Proterozoic asteroid impact ejecta/fallout units and overlying banded iron formations suggests that, in some instances, these impacts were closely followed by significant transformation in the nature of source terrains of the sediments. The Jeerinah Impact Layer (JIL) [B.M. Simonson, D. Davies, S.W. Hassler, Discovery of a layer of probable impact melt spherules in the late Archaean Jeerinah Formation, Fortescue Group, Western Australia. *Aust. J. Earth Sci.* 47 (2000) 315–325; B.M. Simonson, S.W. Hassler, Revised correlations in the early Precambrian Hamersley Basin based on a horizon of resedimented impact spherules. *Aust. J. Earth Sci.* 44 (1997) 37–48; B.M. Simonson, B.P. Glass, Spherule layers — records of ancient impacts. *Ann. Rev. Earth Planet. Sci.* 32 (2004) 329–361; A.Y. Glikson, Early Precambrian asteroid impact-triggered tsunami: excavated seabed, debris flows, exotic boulders, and turbulence features associated with 3.47–2.47 Ga-old asteroid impact fallout units, Pilbara Craton, Western Australia. *Astrobiology* 4 (2001) 19–50; S.W. Hassler, B.M. Simonson, D.Y. Sumner, D. Murphy, Neoarchaean impact spherule layers in the Fortescue and Hamersley Groups, Western Australia: stratigraphic and depositional implications of re-correlation. *Aust. J. Earth Sci.* 52 (2005) 759–772; B. Rasmussen, C. Koeberl, Iridium anomalies and shocked quartz in a late Archaean spherule layer from the Pilbara Craton: new evidence for a major asteroid impact at 2.63 Ga. *Geology* 32 (2004) 1029–1032; B. Rasmussen, T.S. Blake, I.R. Fletcher, U-Pb zircon age constraints on the Hamersley spherule beds: Evidence for a single 2.63 Ga Jeerinah–Carawine impact ejecta layer. *Geology*, 33 (2005) 725–728.] overlies an argillite-dominated unit (Jeerinah Formation, 2684 ± 6 Ma [A.F. Trendall, W. Compston, D.R. Nelson, J.R. deLaeter, V.C. Bennett, SHRIMP zircon ages constraining the depositional chronology of the Hamersley Group, Western Australia. *Aust. J. Earth Sci.* 51 (2004) 621–644.]) and lies directly below a thin volcanic tuff (2629 ± 5 Ma, [A.F. Trendall, W. Compston, D.R. Nelson, J.R. deLaeter, V.C. Bennett, SHRIMP zircon ages constraining the depositional chronology of the Hamersley Group, Western Australia. *Aust. J. Earth Sci.* 51 (2004) 621–644.]) and banded iron formation (BIF) (upper part of Marra Mamba Iron Formation, 2597 ± 5 Ma [A.F. Trendall, W. Compston, D.R. Nelson, J.R. deLaeter, V.C. Bennett, SHRIMP zircon ages constraining the depositional chronology of the Hamersley Group, Western Australia. *Aust. J. Earth Sci.* 51 (2004) 621–644.]). The Spherule Marker Bed (SMB) [B.M. Simonson, Geological evidence for an early Precambrian microtekite strewn field in the Hamersley Basin of Western Australia. *Geol. Soc. Am. Bull.* 104 (1992) 829–839; B.M. Simonson, S.W. Hassler, K.A. Schubel, Lithology and proposed revisions in stratigraphic nomenclature of the Wittenoom Formation (Dolomite) and overlying formations, Hamersley Group, Western Australia. *Geol. Surv. W. Aust. Rep.* 345 (1993) 65–79; S.W. Hassler, B.M. Simonson, D.Y. Sumner, D. Murphy, Neoarchaean impact spherule layers in the Fortescue and Hamersley Groups, Western Australia: stratigraphic and depositional implications of re-correlation. *Aust. J. Earth Sci.* 52 (2005) 759–772. [5]], which includes two impact cycles [A.Y. Glikson, Early Precambrian asteroid impact-triggered tsunami:

Related Articles in ScienceDirect

- [Chapter 8.5 Early Archean Asteroid Impacts on Earth: St... *Developments in Precambrian Geology*](#)
- [Genetic modelling for banded iron-formation of the Hame... *Precambrian Research*](#)
- [Asteroid impact ejecta units overlain by iron-rich sedi... *Earth and Planetary Science Letters*](#)
- [Letter to the editor *Precambrian Research*](#)
- [Bedforms produced by impact-generated tsunami, 2.6 Ga H... *Sedimentary Geology*](#)

[View More Related Articles](#) [Request Permission](#)[View Record in Scopus](#)[Cited By in Scopus \(0\)](#)

excavated seabed, debris flows, exotic boulders, and turbulence features associated with 3.47–2.47 Ga-old asteroid impact fallout units, Pilbara Craton, Western Australia. Astrobiology 4 (2001) 19–50.], is located at the top of a carbonate/calcareous siltstone-dominated sequence (Bee Gorge Member, Wittenoom Formation, 2565 ± 9 Ma [A.F. Trendall, W. Compston, D.R. Nelson, J.R. deLaeter, V.C. Bennett, SHRIMP zircon ages constraining the depositional chronology of the Hamersley Group, Western Australia. Aust. J. Earth Sci. 51 (2004) 621–644.]) and below a carbonate-poor siltstone–chert–BIF sequence (Mount Sylvia Formation, Bruno's Band [BIF], Mount McRae Shale, 2504 ± 5 Ma [B. Rasmussen, T.S. Blake, I.R. Fletcher, U–Pb zircon age constraints on the Hamersley spherule beds: Evidence for a single 2.63 Ga Jeerinah–Carawine impact ejecta layer. Geology, 33 (2005) 725–728.]). No ferruginous sediments overlie impact layers hosted by stromatolitic carbonates (< 2.63 Ga microkrystite spherule-bearing Carawine mega-breccia, east Hamersley Basin; ~ 2.6 –2.65 Ga Monteville impact layer; 2567 Ma Reivilo Formation, west Griqualand Basin, Transvaal) — a lack possibly attributable to enclosed oxygenated high-pH reef environment. Barring a possible presence of undocumented hiatuses between the impact layers and directly overlying units, and within the accuracy limits of U–Pb zircon age data, it follows that the JIL and SMB mega-impacts were succeeded by enhanced supply of ferruginous and clastic materials. The location of 5 out of 8 Archaean to earliest Proterozoic impact fallout/ejecta units below iron-rich sediments [A.Y. Glikson, Asteroid impact ejecta units overlain by iron-rich sediments in 3.5–2.4 Ga terrains, Pilbara and Kaapvaal cratons: Accidental or cause–effect relationships? Earth Planet. Sci. Lett. 246 (2006) 149–160.], including 3.47 Ga, 3.26 Ga, 3.24 Ga, 2.63 Ga and 2.56 Ga units, unless accidental, suggests enrichment of sea water in soluble ferrous iron, possibly derived from impact-triggered mafic volcanic and hydrothermal activity. The scarcity of shocked quartz grains in the ejecta suggests impacts occurred in oceanic regions of the late Archaean Earth [A.Y. Glikson, Early Precambrian asteroid impact-triggered tsunami: excavated seabed, debris flows, exotic boulders, and turbulence features associated with 3.47–2.47 Ga-old asteroid impact fallout units, Pilbara Craton, Western Australia. Astrobiology 4 (2001) 19–50; A.Y. Glikson, Oceanic mega-impacts and crustal evolution, Geology 27 (1999) 341–347; B.M. Simonson, D. Davies, M. Wallace, S. Reeves, S.W. Hassler, Iridium anomaly but no shocked quartz from late Archean microkrystite layer: oceanic impact ejecta? Geology 26 (1998) 195–198.]. Should further examples of sedimentary facies changes associated with large impact events be identified, the impact factor will need to be taken into account in accounting for the crustal transformations during the transition from the end-Archaean to the earliest Proterozoic.

Keywords: asteroid impact; banded iron formation; Pilbara; Hamersley; Western Australia

Article Outline

1. Introduction
 2. Geological setting
 3. Facies variations and correlation of ~ 2.63 Ga impact units
 4. Facies changes associated with 2.56 Ga impact/s
 5. Provenance and depositional environments
 6. Geodynamic consequences
 7. Summary
- Acknowledgements
- References

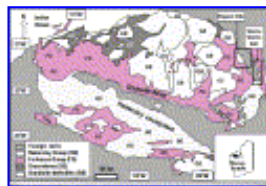
1. Introduction

This paper presents the second part of the documentation and discussion of relationships between impact ejecta/fallout units and associated ferruginous sediments and banded iron formations in early Precambrian terrains [11]. The potential role of large asteroid and comet impacts as triggers of major seismic, tectonic, thermal, magmatic and environmental episodes [12], [13], [14], [15], [16], [17], [18], [19], [20], [21], [22], [23], [24] and [25] remains a fundamental question in Earth science. D.R. Lowe and G.R. Byerly [26] and [27] remarked on the potential significance of the juxtaposition between three 3.26–3.24 Ga impact ejecta/fallout units (S2, S3, S4) in the Barberton Greenstone Belt (BGB), eastern Kaapvaal Craton, South Africa [28], and the abrupt break between ~ 12 km-thick 3.55–3.26 Ga mafic–ultramafic volcanic crust (Onverwacht Group and Mendon Formation) and unconformably overlying < 3.26 Ga turbidite, felsic volcanic and conglomerate-dominated succession (Fig Tree Group, Moodies Group), which includes the earliest observed granite-derived detritus. Clikson and Vickers [29] correlated the BGB impacts with the abrupt change from the ~ 10 km-thick 3.51–3.235 Ga mafic–ultramafic sequence (Warrawoona Group and Sulphur Springs Group) and an overlying < 3.235 Ga turbidite, felsic volcanic, BIF association (Gorge Creek Group) and quartzite–conglomerate sequence (de Gray Group) in the Pilbara Craton. The boundary between these sequences is accompanied by multiple mega-breccia deposits, each overlain by ferruginous sediments. A similar change occurs in the western part of the Pilbara Craton above the 3.27 Ga volcanics of the Ruth Well Formation [29]. Here we focus on the crustal effects of late Archaean 2.63 Ga and 2.56 Ga impacts in the Hamersley Basin, Pilbara Craton, Western Australia, in view of significant contrasts in the nature of sedimentation below and above these impact ejecta/fallout units.

2. Geological setting

The Fortescue Group (2.78–2.63 Ga), northern central Hamersley Basin (Mount Bruce 1:250 000 and Roy Hill 1:250 000 Sheet areas [30] and [31]) consists of a ~ 5600 m-thick succession of basalt (Mount Roe Basalt, Kylena Formation, Maddina Formation), arenite (Hardy Formation), carbonate

and felsic tuff (Tumbiana Formation), and argillite (Jeerinah Formation). The Jeerinah Formation in the Chichester Range ([Fig. 1](#)) consists of \sim 150 m-thick quartz sandstone (Woodiana Formation) overlain by carbonaceous argillite, chert and minor arenite. The overlying Hamersley Group (\sim 2.63–2.45 Ga) consists of \sim 200 m-thick ferruginous chert, banded ironstone and shale (Marra Mamba Iron Formation), 275–700 m-thick carbonate and calcareous siltstone (Wittenoom Formation), \sim 30 m-thick siltstone and ferruginous sediments (Sylvia Formation) capped by BIF (Bruno's Band), \sim 70 m-thick siltstone, ferruginous siltstone and BIF (Mount McRae Shale), and \sim 550 m-thick BIF, ferruginous siltstone, Fe-carbonate (siderite) carbonate and tuff of the Brockman Iron Formation ([Fig. 1](#) and [Fig. 2](#)). The Marra Mamba Formation, which consists of ferruginous chert, banded iron formation and shale, is absent in the eastern part of the Hamersley Basin, where a stromatolitic carbonate (Carawine Dolomite) directly overlies the Jeerinah Formation.



[Display Full Size version of this image \(133K\)](#)

Fig. 1. Geological sketch map of the Pilbara Craton and Hamersley Basin.



[Display Full Size version of this image \(66K\)](#)

Fig. 2. Schematic stratigraphic column for the Hamersley Group, central Hamersley Basin, marking the position and ages of impact ejecta/fallout units (circles) after [\[8\]](#). JIL – Jeerinah impact layer; BGM – Bee Gorge Member; SMB – Spherule Marker Bed; DGS4 – 4th shale macroband of the Dales Gorge Member; BIF – banded iron formation; S – shale.

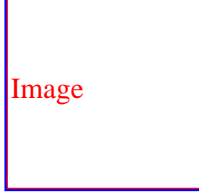
Four impact ejecta/fallout units have been identified and documented in detail by B.M. Simonson, S.W. Hassler and coworkers in the central and eastern parts of the Hamersley Basin, northwest Western Australia ([Fig. 1](#) and [Fig. 2](#)), marked by iridium anomalies [\[32\]](#), [\[33\]](#), [\[34\]](#) and [\[6\]](#) and Cr isotope anomalies [\[35\]](#). These units include:

- (1) The $> 2629 \pm 5$ Ma Jeerinah Impact Layer (JIL) located at the top of the Jeerinah Formation (siltstone, chert, mafic flows and dolerite sills) and below the Marra Mamba Iron Formation (2597 ± 5 Ma [\[8\]](#)).
- (2) The impact spherule-bearing Carawine mega-breccia (CMB) [\[9\]](#), [\[4\]](#) and [\[37\]](#) which overlies argillites including felsic tuff dated as 2630 ± 6 Ma [\[7\]](#).
- (3) The Spherule Marker Bed (SMB) of the Bee Gorge Member, Wittenoom Formation [\[9\]](#), [\[10\]](#) and [\[36\]](#) which overlies felsic tuff dated as 2565 ± 9 Ma [\[8\]](#) and [\[36\]](#).
- (4) The impact fallout unit of the Dales Gorge Member S4 Macroband (DGS4) [\[6\]](#), Brockman Iron Formation (2481 ± 4 Ma [\[8\]](#)), located 37 m above the base of a thick BIF/siltstone sequence.

The stratigraphic relations between these impact ejecta/fallout units and their host stratigraphic units and correlations between the impact layers are discussed in the following sections.

3. Facies variations and correlation of ~ 2.63 Ga impact units

The identification of a 6 mm-thick lamina of microkrystite spherules (Jeerinah Impact Layer – JIL) above the argillite and chert sequence of the Jeerinah Formation at Ilbiana Well was followed by the discovery of an outcrop at Hesta siding (Newman–Port Hedland railway line) [\[1\]](#), [\[2\]](#) and [\[3\]](#). There the JIL comprises an up to 60 cm-thick unit of spherules and spherule-bearing rip-up clast breccia located above argillites and chert of the Jeerinah Formation and overlain by a boulder-size debris flow ([Fig. 3](#)). The age of the JIL is constrained by a U–Pb zircon date of 2629 ± 5 Ma of an overlying volcanic tuff [\[8\]](#) and U–Pb ages on zircon from the base of the underlying Jeerinah Formation (2684 ± 6 Ma [\[38\]](#)). The age of the overlying Marra Mamba Iron Formation is indicated by a U–Pb zircon age for its uppermost member (Mount Newman Member – MNM) of 2597 ± 5 Ma [\[8\]](#) ([Fig. 2](#)). The age Gap of ~ 20 Ma between the JIL and MNM signifies long-term deposition of the ferruginous sediments or, more likely, discontinuous deposition and presence of undetected paraconformities (hiatuses) between the JIL and the banded iron formations or within the Marra Mamba Iron Formation.



Image

[Display Full Size version of this image \(137K\)](#)

Fig. 3. (A) Columnar section of the Jeerinah Impact Layer (JIL) and host sediments (after [4]). Positions of C, D and E photographs are indicated. (B) Railroad-side exposure at Hesta siding, central Pilbara, showing Jeerinah Formation siltstone (JS) and siltstone–chert (JSC), Jeerinah Impact Layer (JIL) and laterite-altered base of the Marra Mamba Iron Formation (M). (C) Boulder debris flow above JIL, containing tabular and rounded decimetre-scale fragments. Swiss knife – 8 cm. (D) Basal rip-up clast breccia of JIL consisting of spherule-rich micro-breccia (white) containing rip-up clasts of ferruginous siltstone (red). Swiss knife – 8 cm. (E) Microscopic view of spherule-rich breccia with rip-up clasts of ferruginous siltstone, showing K-feldspar-rimmed chlorite-cored microkrystite spherules and feldspar-dominated microtekrites (large fragment at the bottom).

A 20–30 m-thick microkrystite and microtekrite-bearing carbonate–chert stratiform mega-breccia unit, identified by Simonson (1992) [9] in the lower part of the Carawine Dolomite, extends over a distance of nearly 100 km northwest–southeast between Ripon Hills and Warrie Warrie Creek, in an eastern outlier of the Hamersley Basin (Fig. 4). The mega-breccia is located about 30–100 m above the contact with underlying siltstone of the Jeerinah Formation, where crystal tuff was dated as 2630 ± 6 Ma [7]. The mega-breccia is either excavated into, or conformably overlies, layered carbonate [4] and [37], and consists of chert and dolomite fragments and up to 7 m-sized blocks derived from the underlying carbonates and from a preexisting chert-rich dolomite unit. Locally the mega-breccia is only about 5–10 m-thick. The top of the mega-breccia pile is marked by several cm-thick lenses of microkrystite spherules and microtekrites. Isolated spherules occur in veins injected into lower stratigraphic levels of the breccia. Carbonate sequences underlying the CMB vary from about 100 m-thick in the Coonanbunna Creek area, northwest Ripon Hills, to about 30 m in the southern part of the Ripon Hills, to about 40 m in the southern part of the Warrie Warrie belt.



Image

[Display Full Size version of this image \(112K\)](#)

Fig. 4. Geological sketch maps of the East Hamersley Basin, indicating distribution of the mega-breccia (CMB) of the Carawine Dolomite (CD). [A] – Ripon Hills; [B] – Warrie Warrie Creek area; KB – Kylena Formation (basalt); MB – Maddina Formation (basalt); JF – Jeerinah Formation; PJ – Pinjian Chert Breccia (silicified surface breccia); WW – Warrie Warrie Creek belt; RH – Ripon Hills. The CMB unit is shown as a thick black line. After [37].

The Carawine mega-breccia was initially regarded as a tsunami facies of the 2.56 Ga Spherule Marker Bed of the central Hamersley Basin due to their dominant carbonate facies and similar isotopic Pb ages [6]. However, unless the Jeerinah Formation and the CMB are separated by an undocumented paraconformity (hiatus), the age overlap between the JIL (2629 ± 5 Ma) and the sub-CMB tuff (2630 ± 6 Ma [7]) requires a correlation between these impact units at a stratigraphic level below a lateral transition from ferruginous sedimentary facies in the central Hamersley Basin (Marra Mamba Iron Formation) to carbonate facies in the eastern Hamersley Basin [2] and [7]. Alternatively, the JIL and CMB represent separate, though geochronologically indistinguishable, impact events. A possible equivalent of the CMB was identified in the Transvaal Group, West Griqualand Basin, South Africa, where an impact layer occurs at lower parts of the thick carbonate sequence of the Monteville Formation $\sim 2.6\text{--}2.65$ [39]. Due to possible existence of undetected paraconformities/hiatuses within stratigraphic sections in both the Hamersley Group and the Transvaal Group, as well as errors inherent in the isotopic ages, the correlation of these units with the Western Australian impact layers remains somewhat uncertain, leaving open the possibility of distinct impact events.

4. Facies changes associated with 2.56 Ga impact/s

The Spherule Marker Bed (SMB) constitutes a unique black-weathering microkrystite and microtekrite-bearing turbidite at the top of the ~ 230 m-thick siltstone–carbonate Bee Gorge Member, Wittenoom Formation. The SMB consists of cm-scale densely packed spherule layers and discontinuous lenses overlain by decimetre-thick graded and cross-layered turbidite units that form a prominent unit of calcareous arenite 12–130 cm-thick capping the carbonate–calcareous siltstone-dominated sequence of the Bee Gorge Member. The maximum age of the SMB is defined by U–Pb ages on an underlying tuff unit [2] dated as 2565 ± 9 Ma [8]. A likely equivalent of the SMB occurs in the Reivilo Formation [39], West Griqualand Basin, Transvaal, located within carbonaceous shale and stromatolitic carbonate about 250–300 m above the Monteville impact layer and dated as 2567 Ma [3]. This closely corresponds to the 2565 ± 9 Ma [8] Spherule Marker Bed.

Further studies suggest that, where complete sections are preserved, the SMB includes two distinct impact cycles, each consisting of a discontinuous basal layer or lenses of spherules overlain by Bouma-cycle turbidites and/or cross-layered tsunami-type calcareous arenite, commonly including turbulence structures [4]. The SMB extends for at least 325 km E–W throughout the Hamersley Basin, over an area $\sim 16\,000$ km², showing

thickness and facies variations from cm-scale layers and discontinuous lenses of densely packed spherules in carbonate–argillite matrix to several decimetre-thick turbidite units with or without dispersed spherules. The thickness of spherule-bearing units generally decreases from north to south and from east to west [9] and [10]. Marked variations were observed between fully developed \sim 1 m-thick spherule-bearing turbidites, comprising two distinct spherule-bearing cycles (SMB-1 and SMB-2), and thin spherule-poor or spherule-free equivalents consisting of one, two or three spherule-bearing and/or spherule-free turbidite units.

Earlier the SMB was assigned to the upper part of the \sim 230 m-thick Bee Gorge Member of the Wittenoom Formation [10]. In the present study, mapping of the SMB along the escarpment between Bee Gorge and Vampire Gorge (Fig. 5) suggests the SMB marks the boundary between contrasted lithological assemblages, including:

(A) An underlying sequence dominated by carbonate and calcareous siltstones, accompanied with minor siltstone, chert, felsic tuff (Bee Gorge Member), with local pockets of intra-formational conglomerate and cross-layered turbidites, including rip-up clasts suggestive of tsunami effects. Sections in the Bee Gorge Member below the SMB have a high ratio of calcareous siltstone to carbonate (\sim 10 at Wittenoom Gorge, Fig. 8), including beds of near-pure carbonate, which include chert intercalations.

(B) An overlying sequence dominated by siltstone, chert, ferruginous chert and minor calcareous sediments, with increasing ferruginous components upward in the sequence (Mount Sylvia Formation). The first few metres of sections overlying the SMB have a ratio of \sim 2.5 calcareous siltstone and siltstone to carbonate, grading upward into less calcareous siltstone and increasingly ferruginous sediments. At Bee Gorge a calcareous bank about 20 m above the SMB represents the stratigraphically uppermost manifestation of carbonate facies.



Image

[Display Full Size version of this image \(138K\)](#)

Fig. 5. Geological sketch map of the Hamersley escarpment (see Fig. 1 for location) between Vampire Gorge and Bee Gorge. WF – Wittenoom Formation; SM – Mount Sylvia Formation and Mount McRae Shale; BIF – Brockman Iron Formation. The Spherule Marker Bed (SMB) defines the boundary between the WF and SM. The impact unit located at the top of the 4th shale macroband of the Dales Gorge Member (DGS4) occurs 37 m above the base of the Dales Gorge Member.

These field relations are illustrated for the Bee Gorge section (Fig. 6) and Vampire Gorge section (Fig. 7), and on a finer scale for the Wittenoom Gorge and Munjina Gorge sections (Fig. 8).



Image

[Display Full Size version of this image \(194K\)](#)

Fig. 6. Bee Gorge section (see Fig. 5 for location). Columnar section and outcrops of the Bee Gorge Member (BGM) of the Wittenoom Formation, Spherule Marker Bed (SMB) and Mount Sylvia Formation; C – carbonate; M – marl and calcareous siltstone; H – chert; S – siltstone; F – ferruginous siltstone and chert. (A) A view of Bee Gorge Creek section east of the opening of Bee Gorge. Arrow points to the location of the SMB. (B) Outcrop of the SMB overlain by siltstone, ferruginous siltstone and minor carbonate. The brown bank at mid-distance is the uppermost carbonate unit in the section, overlain by ferruginous siltstone and Fe-chert. (C) Bee Gorge Member: calcareous siltstone (marl) including a carbonate layer (white). (D) Bee Gorge Member: carbonates (grey layers) and calcareous siltstone (red). (E) SMB: microkrystite spherule-bearing cross layered turbidite. (F) Mount Sylvia Formation: Fe-chert layers (black) within ferruginous siltstone.



Image

[Display Full Size version of this image \(210K\)](#)

Fig. 7. Vampire Gorge section (see Fig. 5 for location). Columnar section and outcrops of the Bee Gorge Member (BGM) west of Vampire Gorge; Spherule Marker Bed (SMB) and Mount Sylvia Formation; C – carbonate; M – marl and calcareous siltstone; H – chert; S – siltstone; F – ferruginous siltstone and chert; V – volcanic tuff. (A) View of section. Arrow points to position of the SMB. (B) Bee Gorge Member: carbonate banks separated by calcareous siltstone. (C) Bee Gorge Member: calcareous siltstone and carbonate layers (grey). (D) SMB: rhythmically layered turbidites associated with the SMB. (E) SMB: rip-up carbonate clasts

associated with the SMB. (F) Mount Sylvia Formation: ferruginous siltstone and Fe–chert. (G) Mount Sylvia Formation: cliff-forming Fe–chert and ferruginous siltstone.



[Display Full Size version of this image \(102K\)](#)

Fig. 8. Columnar sections of the Spherule Marker Bed, including SMB-1 and SMB-2, at Munjina Gorge (AMG 50K 673584E7520756N), Cathedral Pool and Crossing Pool (50K 636214E7533408N) at Wittenoom Gorge. CM[S] – carbonate + marl + minor siltstone; SM[C] – siltstone + marl + minor carbonate; SF[C] – siltstone + ferruginous siltstone + minor carbonate; M/C – ratio of marl (calcareous siltstone) to carbonate; S/C – ratio of calcareous siltstone and siltstone to carbonate.

5. Provenance and depositional environments

The succession of the late Archaean mega-impacts by major banded iron formations and, for the 2.56 Ga event, with increased clastic sedimentation, is suggestive of major enrichment of sea water in soluble ferrous iron, requiring explanation of its source. Thus, the Marra Mamba Iron Formation almost directly overlies the debris flow unit which caps the JIL impact layer (Fig. 3). The Spherule Marker Bed (SMB) coincides with a transition from carbonate and calcareous siltstone-dominated sequence to a siltstone and ferruginous siltstone-dominated sequence, followed by BIFs of the Bruno's Band (Fig. 6, Fig. 7 and Fig. 8). Barring the existence of undocumented paraconformities/hiatuses between the impact layers and the overlying BIF and clastic sediments/BIF association, it follows that iron enrichment was temporally associated with and thus possibly related to the impact events. By contrast, the absence of ferruginous enrichment above the spherule-bearing Carawine mega-breccia, east Hamersley Basin, and the Monteville and Reivilo impact layers [39], Transvaal, may be related to the stromatolitic nature of the host Carawine Dolomite, Monteville Formation and Reivilo Formation, which likely formed in partly protected shallow reef environments where alkaline high pH conditions, and possibly photosynthetic oxygen, would result in conditions distinct from those where banded iron formations form.

An interpretation of the origin of sea water iron enrichment above 3.47 Ga, 3.26 Ga, 3.24 Ga 2.63 Ga and 2.56 Ga impact layers and associated tsunami deposits [4] and [36] in terms of the denudation of mafic volcanics and of Fe-rich hydrothermal activity triggered by the impacts [11], while unproven, is amenable to further field tests and isotopic studies. The onset of detrital sedimentation following the 3.26 Ga, 3.24 Ga and 2.56 Ga events suggests rejuvenation of source terrains of clastic sediments, possibly due to impact-triggered seismic faulting. Mantle isotopic signatures recorded in banded iron formations of the Hamersley Basin include positive ϵ_{Nd} values ($+1.0 \pm 0.5$) whereas associated shale bands yield mixed continental-oceanic ϵ_{Nd} signatures (-0.9 ± 0.6) [40]. Iron isotope $^{56}\text{Fe}/^{54}\text{Fe}$ signatures cluster about the igneous field, with departures attributed to diagenetic changes [41]. An alternation between volcanic or hydrothermal sources of the iron-rich bands and continental weathering sources of silica bands is supported by Ge/Si trace element studies [42]. The waning of carbonate sedimentation of the Bee Gorge Member of the Wittenoom Formation and onset of BIF and chert deposition reflects changes in seawater chemistry, from high pH conditions which allow carbonate (+minor chert) precipitation to low pH conditions allowing transport of ferrous iron. Such changes would be accompanied by fluctuations between moderate Eh, which allows oxidation of Fe^{+2} to Fe^{+3} , and low Eh conditions required for deposition of reduced black shale of the Mount Sylvia Formation and Mount McRae Formation. Microbial mediation of iron oxidation is supported by precise correlations of iron-silica microbands throughout the Hamersley Basin [43], [44], [45], [46], [47], [48], [49] and [50].

6. Geodynamic consequences

To date, suggested cause-effect relations between large asteroid/comet impacts and igneous, tectonic or plate tectonic events [12], [13], [14], [15], [16], [17], [18], [24] and [25] have not been accompanied with direct field evidence. Ivanov and Melosh, 2003 [23] placed constraints on the likelihood of impact-triggered volcanic activity, referring to it as a rare coincidence in Earth history. However, these authors also state: "Indeed, a few giant impact events certainly occurred on Earth in post-Late Heavy Bombardment (LHB: 3.95–3.85 Ga) history, and a few might have encountered the fortuitous circumstances necessary for them to enhance magma production". The likelihood of impact-triggered volcanism is significantly higher in geothermally active oceanic crustal regions. For an impact flux of craters of $D_s > 20 \text{ km}$ (D_s = outer diameter) of the order of $4.3\text{--}6.3 \times 10^{-15}$ impacts $\text{km}^{-2} \text{ yr}^{-1}$ [51] on a post-3.8 Ga Earth occupied by > 80% time-integrated oceanic crust [52], assuming a cumulative asteroid and crater size/frequency distribution $N_D \propto D^{10-1.8}$ (N_D = number of craters of diameter D), ~ 360 craters with $D > 100 \text{ km}$ and ~ 40 craters with $D > 300 \text{ km}$ would form in oceanic basins [22]. A steeper size/frequency distribution of $N_D \propto D^{10-2.2}$ [53] would result in 125–250 craters of $D > 100 \text{ km}$ and 6–12 craters of $D > 300 \text{ km}$. From this estimate, in so far as the 3.26 Ga, 3.24 Ga, 2.63 Ga, 2.56 Ga, 2.48 Ga, $\sim 2.02 \text{ Ga}$ (Vredefort) and 1.85 Ga (Sudbury) mega-impacts correspond to craters of $D \geq 300 \text{ km}$, it follows that about half the number of very large post-LHB impacts on Earth have at this stage been identified.

Compared to the present-day mid-ocean geotherm of $25^\circ \text{C km}^{-1}$ over areas $\sim 10\%$ of oceanic basins, assuming similar or higher Archean geothermal gradients and possibly smaller-scale convection cells and plate dimensions [54], large sectors of Archean oceanic crustal regions would be underlain by thin ($\sim 5 \text{ km}$) basaltic crust and shallow ($< 50 \text{ km}$) asthenosphere. Whereas low angle impacts would be partly absorbed by deep

water columns, high-angle impacts by asteroids $\sim 10\text{--}20$ km-large would result in submarine craters on the scale of several hundred kilometres. As originally modeled [12] and [13] downward compression of the transient crater followed by rebound of asthenosphere originally located at $\sim 40\text{--}50$ km would result in intersection of the peridotite solidus by rising partially molten mantle diapirs (Fig. 9). In so far as morphometric estimates [55] apply to asthenospheric uplift the amount of rebound may be similar to that of a central uplift $SU = 0.086D_s^{1.03}$, namely ~ 30 km. However, such large rebound, deduced from craters formed in the crust, may not apply to dense viscous mantle [23].



Image

[Display Full Size version of this image \(99K\)](#)

Fig. 9. Pressure–temperature diagram portraying the position of the lithosphere–asthenosphere boundary for continental and oceanic geotherms and the position of dry and wet peridotite solidi [13]. Downward arrow marks the ~ 30 km penetration depth of a 20 km asteroid, equivalent to decompression. Upward arrows mark alternative adiabatic melting paths of mantle diapirs (adiabatic cooling $0.33\text{ }^{\circ}\text{C}/\text{km}$).

Models of the magmatic consequences of very large impacts [24] and [25], suggest that a ~ 300 km-radius crater excavating 75 km-thick lithosphere will produce 10^6 km^3 of magma through instantaneous in-situ decompression of the mantle and updoming of the asthenosphere, triggering longer-term mantle convection and adiabatic melting, in particular under high geothermal gradients. These volumes are similar to those estimated by Ivanov and Melosh [23]. The short eruption spans of large volumes of some plateau basalts (Deccan: 2.10^6 km^3 in 0.3 Ma; Emeishan: 9.10^5 km^3 in 0.3 Ma; Siberian: $3\text{--}4.10^6\text{ km}^3$ in 0.4 Ma) are consistent with volumes deduced by these authors for excavation of large-radii impact craters. Impacts on this magnitude would have world-wide effects for which ample evidence could remain in the rock record. [25].

Jones et al., 2005 [17] conducted hydrocode simulations to test whether impact triggered volcanism is consistent with the origin of the Ontong–Java Plateau, using dry lherzolite melting parameters, a steep oceanic geotherm and a vertical incidence by a dunite projectile (diameter 30 km: velocity 20 km/s). The thermal and physical state of target lithosphere is critical for estimates of melt production. Model calculations suggest impact-triggered melting in a sub-horizontal disc of ~ 600 km-diameter down to > 150 km-depth in the upper mantle forms within ~ 10 min of the impact, whereas most of the initial melt forms at depths shallower than ~ 100 km. The volume of ultramafic melt would reach $\sim 2.5 \times 10^6\text{ km}^3$, ranging from superheated melts within 100 km of ground zero to partial melting with depth and distance. The total melt volume would reach $\sim 7.5 \times 10^6\text{ km}^3$ of basalt if heat was distributed to produce 20–30% partial mantle melting.

The late Archaean impact units provide further support for Lowe et al.'s (1989) [26] original observation of the tectonic significance of the S2–S4 Barberton impacts, which are juxtaposed with the fundamental break between the $\sim 3.55\text{--}3.26$ Ga Onverwacht Group (mafic–ultramafic volcanic sequence) and the overlying Fig Tree Group (turbidite–felsic volcanic-banded iron formation association), also observed in the Pilbara Craton, Western Australia [29]. It may follow that the 3.26–3.24 Ga impact cluster resulted in an abrupt termination of the protracted evolution of greenstone–TTG (tonalite–trondhjemite–granodiorite) systems, faulting, vertical movements and unconformities, and was accompanied by volcanic activity (Sulphur Springs Group, central Pilbara Craton) and major plutonic magmatism in the Kaapvaal Craton (Nelshoogte and Kaap Valley plutons) and the Pilbara Craton (Cleland plutonic suite). Iridium and chrome isotope-based mass balance calculations, spherule size analysis and the ferromagnesian composition of the impact ejecta suggest asteroids about 20–50 km-diameter resulting in impact basins on the scale of 200–1000 km-diameter excavated in mafic–ultramafic crustal regions of the Archaean Earth. The evidence presented in this paper on the relationships between late Archaean impact layers and overlying ferruginous siltstone and BIF lend further support for re-evaluation of the role of asteroid and comet impacts in Earth history.

7. Summary

This paper presents evidence for the succession of late Archaean impact event horizons – marked by microkrystite and microtektite-bearing ejecta/fallout units and associated turbidites and tsunami deposits – by ferruginous siltstone and banded iron formation. Impact units include the ~ 2.63 Ga Jeerinah Impact layer (JIL) and the ~ 2.56 Ga Spherule Marker Bed (SMB). Principal observations include:

1. The ~ 2.63 Ga JIL [1], [2] and [3] is directly overlain by debris flow boulder deposit, capped by a thin tuff unit directly overlain by the Marra Mamba Iron Formation.
2. The ~ 2.56 Ga Spherule Marker Bed (SMB) [9] and [10], regarded as a double impact [4], marks a transition from an underlying calcareous siltstone–carbonate assemblage to an overlying carbonate-poor assemblage of siltstone, ferruginous siltstone, Fe–chert and banded iron formation.
3. The stromatolitic carbonate-dominated post-2.63 Ga microkrystite and microtektite-rich Carawine mega-breccia (CMB) [7], and the Monteville (2.6–2.65 Ga) and Reivilo (2.567 Ga) impact layers, are not succeeded by ferruginous sediments, an absence possibly interpreted in terms of enclosed high-pH oxygenated reef environments.

4. The succession of 2.63 Ga and 2.56 Ga impact ejecta/fallout units by ferruginous or ferruginous/clastic sediments is consistent with relations observed in 3.47 Ga, 3.26 Ga and 3.24 Ga impact units [11].
5. The relationships between impact events and the onset of ferruginous, and in some instances clastic and ferruginous, sedimentation, require contemporaneous enrichment of sea water in ferrous iron, possibly hinting at provenance mafic volcanic activity, consistent with models advocating impact-triggered igneous activity [12], [13], [14], [15], [16], [17], [18], [19], [20], [21], [22], [23], [24] and [25].
6. Isotopic age gaps between and within lithostratigraphic units of the Fortescue Group and Hamersley Group (Fig. 2) leave open the possible existence of hiatuses (paraconformities) between the impact ejecta/fallout units and overlying ferruginous and detrital sediments. Further isotopic age determinations of units below and above the impact horizons are required in order to elucidate this question.

Acknowledgements

We thank Steve Drury for the constructive review, and Richard Morris, Keith Crook, Allastair Stewart and Patrick DeDeckker for the comments on the manuscript. We are grateful to Arthur Hickman, Martin Van Kranendonk, Franco Pirajno and other members of the Geological Survey of Western Australia for their support of this research, and to Peter Morant, Mike Doepel and Carl Brauhart of SIPA Resources Ltd for help and discussions.

References

- [1] B.M. Simonson, D. Davies and S.W. Hassler, Discovery of a layer of probable impact melt spherules in the late Archean Jeerinah Formation, Fortescue Group, Western Australia, *Aust. J. Earth Sci.* **47** (2000), pp. 315–325. [Full Text via CrossRef](#) | [View Record in Scopus](#) | [Cited By in Scopus \(20\)](#)
- [2] B.M. Simonson and S.W. Hassler, Revised correlations in the early Precambrian Hamersley Basin based on a horizon of resedimented impact spherules, *Aust. J. Earth Sci.* **44** (1997), pp. 37–48. [Full Text via CrossRef](#) | [View Record in Scopus](#) | [Cited By in Scopus \(32\)](#)
- [3] B.M. Simonson and B.P. Glass, Spherule layers — records of ancient impacts, *Annu. Rev. Earth Planet. Sci.* **32** (2004), pp. 329–361. [Full Text via CrossRef](#) | [View Record in Scopus](#) | [Cited By in Scopus \(24\)](#)
- [4] A.Y. Glikson, Early Precambrian asteroid impact-triggered tsunami: excavated seabed, debris flows, exotic boulders, and turbulence features associated with 3.47–2.47 Ga-old asteroid impact fallout units, Pilbara Craton, Western Australia, *Astrobiology* **4** (2001), pp. 19–50.
- [5] S.W. Hassler, B.M. Simonson, D.Y. Sumner and D. Murphy, Neoarchaean impact spherule layers in the Fortescue and Hamersley Groups, Western Australia: stratigraphic and depositional implications of re-correlation, *Aust. J. Earth Sci.* **52** (2005), pp. 759–772.
- [6] B. Rasmussen and C. Koeberl, Iridium anomalies and shocked quartz in a late Archean spherule layer from the Pilbara Craton: new evidence for a major asteroid impact at 2.63 Ga, *Geology* **32** (2004), pp. 1029–1032. [Full Text via CrossRef](#) | [View Record in Scopus](#) | [Cited By in Scopus \(10\)](#)
- [7] B. Rasmussen, T.S. Blake and I.R. Fletcher, U–Pb zircon age constraints on the Hamersley spherule beds: evidence for a single 2.63 Ga Jeerinah–Carawine impact ejecta layer, *Geology* **33** (2005), pp. 725–728. [Full Text via CrossRef](#) | [View Record in Scopus](#) | [Cited By in Scopus \(3\)](#)
- [8] A.F. Trendall, W. Compston, D.R. Nelson, J.R. deLaeter and V.C. Bennett, SHRIMP zircon ages constraining the depositional chronology of the Hamersley Group, Western Australia, *Aust. J. Earth Sci.* **51** (2004), pp. 621–644. [Full Text via CrossRef](#) | [View Record in Scopus](#) | [Cited By in Scopus \(11\)](#)
- [9] B.M. Simonson, Geological evidence for an early Precambrian microtektite strewn field in the Hamersley Basin of Western Australia, *Geol. Soc. Amer. Bull.* **104** (1992), pp. 829–839. [View Record in Scopus](#) | [Cited By in Scopus \(40\)](#)
- [10] B.M. Simonson, S.W. Hassler and K.A. Schubel, Lithology and proposed revisions in stratigraphic nomenclature of the Wittenoom Formation (Dolomite) and overlying formations, Hamersley Group, Western Australia, *Rep.-Geol. Surv. West. Aust.* **345** (1993), pp. 65–79.
- [11] A.Y. Glikson, Asteroid impact ejecta units overlain by iron-rich sediments in 3.5–2.4 Ga terrains, Pilbara and Kaapvaal cratons: accidental or cause–effect relationships?, *Earth Planet. Sci. Lett.* **246** (2006), pp. 149–160. [SummaryPlus](#) | [Full Text + Links](#) | [PDF \(974 K\)](#) | [View Record in Scopus](#) | [Cited By in Scopus \(3\)](#)
- [12] D.H. Green, Archaean greenstone belts may include terrestrial equivalents of lunar maria?, *Earth Planet. Sci. Lett.* **15** (1972), pp. 263–270.

[Abstract](#) | [PDF \(645 K\)](#)

[13] D.H. Green, Petrogenesis of Archaean ultramafic magmas and implications for Archaean tectonics. In: A. Kröner, Editor, *Precambrian Plate Tectonics*, Elsevier, Amsterdam (1981), pp. 469–489.

[14] R.A.F. Grieve, Impact bombardment and its role in proto-continental growth of the early Earth, *Precambrian Res.* **10** (1980), pp. 217–248. [View Record in Scopus](#) | [Cited By in Scopus \(12\)](#)

[15] H.G. Hughs, F.N. App and T.N. McGetchin, Global seismic effects of basin-forming impacts, *Phys. Earth Planet. Inter.* **15** (1977), pp. 251–263.

[16] A.G. Jones, Are impact-generated lower crustal faults observable, *Earth Planet. Sci. Lett.* **85** (1987), pp. 248–252. [Abstract](#) | [PDF \(347 K\)](#) | [View Record in Scopus](#) | [Cited By in Scopus \(3\)](#)

[17] A.P. Jones, K. Wünemann and G.D. Price, Modeling impact volcanism as a possible origin for the Ontong Java Plateau, *Geol. Soc. Am., Spec. Pap.* **388** (2005), pp. 711–720. [Full Text via CrossRef](#)

[18] A.D. Alt, J.W. Sears and D.W. Hyndman, Terrestrial maria: the origins of large basalt plateaus, hotspot tracks and spreading ridges, *J. Geol.* **96** (1988), pp. 647–662.

[19] V.R. Oberbeck, J.R. Marshall and H. Aggarwal, Impacts, tillites and the breakdown of Gondwanaland, *J. Geol.* **101** (1992), pp. 1–19.

[20] M.B. Boslough, E.P. Chael, T.G. Trucano, M.E. Kipp and D.A. Crawford, Axial focussing of impact energy in the Earth's interior: proof-of-principle tests of a new hypothesis, *Lunar Planetary Institution Contribution* **825** (1994), pp. 14–15.

[21] A.Y. Glikson, Oceanic mega-impacts and crustal evolution, *Geology* **27** (1999), pp. 341–387.

[22] A.Y. Glikson, The astronomical connection of terrestrial evolution: crustal effects of post-3.8 Ga mega-impact clusters and evidence for major 3.2 ± 0.1 Ga bombardment of the Earth–Moon system, *J. Geodyn.* **32** (2001), pp. 205–229. [SummaryPlus](#) | [Full Text + Links](#) | [PDF \(2481 K\)](#) | [View Record in Scopus](#) | [Cited By in Scopus \(21\)](#)

[23] B.A. Ivanov and H.J. Melosh, Impacts do not initiate volcanic eruptions: eruptions close to the crater, *Geology* **31** (2003), pp. 869–872. [Full Text via CrossRef](#) | [View Record in Scopus](#) | [Cited By in Scopus \(24\)](#)

[24] L.T. Elkin-Tanton, B.H. Hager and T.L. Grove, Magmatic effects of the lunar late heavy bombardment, *Earth Planet. Sci. Lett.* **222** (2004), pp. 17–27.

[25] L.T. Elkin-Tanton, Giant meteoroid impacts can cause volcanism, *Earth Planet. Sci. Lett.* **239** (2005), pp. 219–232.

[26] D.R. Lowe, G.R. Byerly, F. Asaro and F.T. Kyte, Geological and geochemical record of 3400 Million years old terrestrial meteorite impacts, *Science* **24** (1989), pp. 959–962. [View Record in Scopus](#) | [Cited By in Scopus \(35\)](#)

[27] D.R. Lowe and G.R. Byerly, Tectonic and sedimentological effects of large 3250 million years old meteorite impacts, Barberton greenstone belt, *Abstr. Annu. Meet. Geol. Soc. Am.* (1990).

[28] D.R. Lowe, G.R. Byerly, F.T. Kyte, A. Shukolyukov, F. Asaro and A. Krull, Spherule beds 3.47–3.34 Ga-old in the Barberton Greenstone Belt, South Africa: a record of large meteorite impacts and their influence on early crustal and biological evolution, *Astrobiology* (2003), pp. 7–48.

[29] A.Y. Glikson and J. Vickery, The 3.26–3.24 Ga Barberton asteroid impact cluster: Tests of tectonic and magmatic consequences, Pilbara Craton, Western Australia, *Earth Planet. Sci. Lett.* **241** (2006), pp. 11–20. [SummaryPlus](#) | [Full Text + Links](#) | [PDF \(841 K\)](#) | [View Record in Scopus](#) | [Cited By in Scopus \(3\)](#)

[30] A.M. Thorne and I.M. Tyler, Mount Bruce 1:250 000 geological map with explanatory notes, *Geol. Surv. West. Aust.* (1997), p. 28.

[31] A.M. Thorne and I.M. Tyler, Roy Hill 1:250 000 geological map with explanatory notes, *Geol. Surv. West. Aust.* (1997), p. 22.

[32] B.M. Simonson, D. Davies, M. Wallace, S. Reeves and S.W. Hassler, Iridium anomaly but no shocked quartz from late Archean microkrystite layer: oceanic impact ejecta?, *Geology* **26** (1998), pp. 195–198. [Full Text via CrossRef](#) | [View Record in Scopus](#) | [Cited By in Scopus \(30\)](#)

- [33] I. McDonald and B.M. Simonson, PGE anomalies detected in two more 2.5–2.6 billion years-old spherule layers in the Hamersley Basin of Western Australia, *Lunar Planet. Sci.* **33** (2002), p. 3.
- [34] A.Y. Glikson and C. Allen, Multiple c. 3.47 Ga-old asteroid impact fallout units, Pilbara Craton, Western Australia, *Earth Planet. Sci. Lett.* **221** (2004), pp. 383–396. [SummaryPlus](#) | [Full Text + Links](#) | [PDF \(1540 K\)](#) | [View Record in Scopus](#) | [Cited By in Scopus \(8\)](#)
- [35] A. Shukolyukov, P. Castillo, B.M. Simonson and G.W. Lugmair, Chromium in Late Archean spherule layers from Hamersley Basin, Western Australia: isotopic evidence for extra-terrestrial component, *Lunar Planet. Sci.* **33** (2002), p. 1369 abs. 1369 (CD-ROM).
- [36] S.W. Hassler and B.M. Simonson, The sedimentary record of extraterrestrial impacts in deep shelf environments: evidence from the early Precambrian, *J. Geol.* **109** (2001), pp. 1–19. [Full Text via CrossRef](#) | [View Record in Scopus](#) | [Cited By in Scopus \(21\)](#)
- [37] I.R. Williams, Yilgalong 1:1 000 000 Geological Sheet No. 3055, Western Australia: Western Australia Geological Survey, 1:100 000 Geological Series, 2005.
- [38] N.T. Arndt, D.R. Nelson, W. Compston, A.F. Trendall and A.M. Thorne, The age of the Fortescue Group, Hamersley Basin, Western Australia, from ion microprobe zircon U–Pb results, *Aust. J. Earth Sci.* **38** (1991), pp. 261–281. [Full Text via CrossRef](#) | [View Record in Scopus](#) | [Cited By in Scopus \(90\)](#)
- [39] B.M. Simonson, D.Y. Sumner, N.J. Beukes, S. Hassler, I. Kohl, S. Jones-Zimberlin, S. Johnson, A. Scally and J. Gutzmer, Correlating multiple Neoarchaean–Palaeoproterozoic impact spherule layers between South Africa and Western Australia, *Lunar Planet. Sci.* **XXXVII** (2006) 1489 pdf.
- [40] C. Alibert and M.T. McCulloch, Rare earth element and neodymium composition of the banded iron-formations and associated shales from Hamersley, Western Australia, *Geochim. Cosmochim. Acta* **57** (1993), pp. 187–204. [Abstract](#) | [Abstract + References](#) | [PDF \(2837 K\)](#) | [View Record in Scopus](#) | [Cited By in Scopus \(52\)](#)
- [41] B.L. Beard, C.M. Johnson, J.L. Skulan, K.H. Nealson, L. Cox and H. Dun, Application of Fe isotopes to tracing the geochemical and biological cycling of Fe, *Chem. Geol.* **195** (2003), pp. 87–117. [SummaryPlus](#) | [Full Text + Links](#) | [PDF \(683 K\)](#) | [View Record in Scopus](#) | [Cited By in Scopus \(105\)](#)
- [42] T. Hamade, K.O. Konhauser, R. Raiswell, S. Goldsmith and R.C. Morris, Using Ge/Si ratios to decouple iron and silica fluxes in Precambrian banded iron-formations, *Geology* **31** (2003), pp. 35–38. [Full Text via CrossRef](#) | [View Record in Scopus](#) | [Cited By in Scopus \(10\)](#)
- [43] A.F. Trendall and J.G. Blockley, The iron-formations of the Precambrian Hamersley Group, Western Australia: with special reference to associated crocidolite, *Geol. Surv. West. Aust., Bull.* **119** (1970), p. 336.
- [44] P. Cloud, Paleoecological significance of the banded iron formation, *Econ. Geol.* **68** (1973), pp. 1135–1143.
- [45] H.D. Holland, The oceans: a possible source of iron in iron formations, *Econ. Geol.* **68** (1973), pp. 1169–1172.
- [46] H.L. James and A.F. Trendall, Banded iron-formation: distribution in time and paleo-environmental significance. In: H.D. Holland and M. Schidlowski, Editors, *Mineral Deposits and the Evolution of the Biosphere*, Springer–Verlag, New York (1982), pp. 199–218.
- [47] W.E. Ewers and R.C. Morris, Studies of the Dales Gorge Member of the Brockman Iron Formation, Western Australia, *Econ. Geol.* **76** (1981), pp. 1929–1953. [View Record in Scopus](#) | [Cited By in Scopus \(32\)](#)
- [48] R.C. Morris and R. Horwitz, The origin of the iron-formation-rich Hamersley Group of Western Australia — deposition on a platform, *Precambrian Res.* **21** (1983), pp. 197–273.
- [49] R.C. Morris, Genetic modelling for banded iron-formation of the Hamersley Group, Pilbara Craton, Western Australia, *Precambrian Res.* **60** (1993), pp. 243–286. [Abstract](#) | [Abstract + References](#) | [PDF \(3860 K\)](#) | [View Record in Scopus](#) | [Cited By in Scopus \(59\)](#)
- [50] K.O. Konhauser, T. Hamada, R. Raiswell, R.C. Morris, F. Ferris, G. Southam and D. Canfield, Could bacteria have formed the Precambrian banded iron-formations?, *Geology* **30** (2002), pp. 1079–1082. [Full Text via CrossRef](#) | [View Record in Scopus](#) | [Cited By in Scopus \(43\)](#)
- [51] E.M. Shoemaker and C.S. Shoemaker, The Proterozoic impact record of Australia, *AGSO J. Aust. Geol. Geophys.* **16** (1996), pp. 379–398. [View](#)

[Record in Scopus](#) | [Cited By in Scopus \(45\)](#)

[52] M.T. McCulloch and V.C. Bennett, Progressive growth of the Earth's continental crust and depleted mantle: geochemical constraints, *Geochim. Cosmochim. Acta* **58** (1994), pp. 4717–4738. [Abstract](#) | [Abstract + References](#) | [PDF \(3240 K\)](#) | [View Record in Scopus](#) | [Cited By in Scopus \(110\)](#)

[53] G. Neukum, B. Ivanov and W.K. Hartmann, Cratering records in the inner solar system. In: R. Kallenbach *et al.*, Editors, *Chronology and Evolution of Mars*, Kluwer, Dordrecht (2001), pp. 55–86.

[54] R.St.J. Lambert, Archaean thermal regimes, crustal and upper mantle temperatures, and a progressive evolutionary model for the Earth. In: B.F. Windley, Editor, *The Early History of the Earth*, John Wiley & Sons, London (1975), pp. 363–376.

[55] R.A.F. Grieve and M. Pilkington, The signature of terrestrial impacts, *AGSO J. Aust. Geol. Geophys.* **16** (1996), pp. 399–420. [View Record in Scopus](#) | [Cited By in Scopus \(63\)](#)

 Corresponding author. Tel./fax: +61 2 6296 3853.

Earth and Planetary Science Letters

Volume 254, Issues 1-2, 15 February 2007, Pages 214-226

[Home](#) [Browse](#) [Search](#) [My Settings](#) [Alerts](#) [Help](#)



[About ScienceDirect](#) | [Contact Us](#) | [Terms & Conditions](#) | [Privacy Policy](#)

Copyright © 2007 Elsevier B.V. All rights reserved. ScienceDirect® is a registered trademark of Elsevier B.V.

